Polymer Journal (2019) 51:489–499
https://doi.org/10.1038/s41428-018-0164-1

ORIGINAL ARTICLE

Surface-functionalization of isotactic polypropylene via dip-coating with a methacrylate-based terpolymer containing perfluoroalkyl groups and poly(ethylene glycol)

Manami Hara[1] · Shigeru Kitahata[1] · Keisuke Nishimori[1] · Koki Miyahara[1] · Kenta Morita[2] · Kaya Tokuda[1] · Takashi Nishino[1] · Tatsuo Maruyama[1]

Received: 30 September 2018 / Revised: 15 November 2018 / Accepted: 30 November 2018 / Published online: 9 January 2019

Abstract

Isotactic polypropylene (PP) is one of the most popular plastics. However, the remarkably low surface energy of PP prevents the surface functionalization of PP. We studied the surface functionalization of PP by dip-coating with a maleic anhydride-grafted chlorinated polypropylene (MPO)/methacrylate-based terpolymer mixture. A methacrylate-based terpolymer (PMFP) was synthesized, which contained perfluoroalkyl (R_f)-conjugated monomers and poly(ethylene glycol)-conjugated monomers. Tape-peeling tests revealed that MPO successfully immobilized PMFP on a PP surface, although PMFP was less adhesive to PP. X-ray photoelectron spectroscopy (XPS), contact angle, and protein adsorption measurements revealed that the R_f groups and PEG chains in PMFP were segregated to the outermost surface of the dip-coated layer. The surface segregation of these moieties produced a low-fouling surface on the PP substrate. In addition, we synthesized a terpolymer that contained R_f groups and PEG chains with carboxy groups at their termini (PMFB) and used it to dip-coat a PP substrate. The surface segregation of side chains in PMFB induced the presentation of carboxy groups at the outermost surface, which were used as reactive sites for enzyme immobilization.

Introduction

The surface properties of solid materials, e.g., hydrophobicity, wettability, reactivity, antifouling properties, and cell adhesiveness, play important roles in many industrial and household applications [1–8]. Since the last century, the use of polymeric materials, particularly plastics, in a broad range of commodity products, as well as in the automotive and building industries, has been increasing due to their low manufacturing cost, low weight, tunable mechanical properties, and good processability. Isotactic polypropylene (PP) is one of the most popular plastics used in applications that require high chemical and heat resistance, as well as high mechanical strength. Indeed, the market for PP is extremely large and continues to grow (US$ 71.08 billion in 2016) [9, 10] (https://www.marketsandmarkets.com/Market-Reports/polypropylene-market-64103589.html) and includes packaging, textiles, containers, automotive parts, laboratory apparatus, and medical devices. The surface functionalization of PP is important in industry and in the development of novel PP-based devices. However, PP has a remarkably low surface energy because, as is evident from its chemical structure, it consists of only hydrocarbons [11], meaning that it does not show significant adhesiveness or reactivity toward other molecules [12]. Although several approaches (e.g., plasma [13, 14], flame [15], and etching oxidation [16]) for the modification of PP surfaces have

These authors contributed equally to this study: Manami Hara, Shigeru Kitahata.

Supplementary information The online version of this article (https://doi.org/10.1038/s41428-018-0164-1) contains supplementary material, which is available to authorized users.

✉ Tatsuo Maruyama
tmarutcm@crystal.kobe-u.ac.jp

[1] Department of Chemical Science and Engineering, Graduate School of Engineering, Kobe University, 1-1 Rokkodai, Nada-ku, Kobe 657-8501, Japan

[2] Instrumental Analysis Division, Research Facility Center for Science and Technology, Kobe University, 1-1 Rokkodai, Nada-ku, Kobe 657-8501, Japan

been reported [17–21], they require special apparatus, and are not applicable to PP substrates with complicated structures [22–26]. Despite the long history of PP, there is still a high demand for a novel and versatile method of surface functionalization. Rojas and colleagues [27] used protein adsorption to make the surface of a PP fiber hydrophilic, and Ishihara and colleagues [28] succeeded in the suppression of blood cell adhesion to a PP surface using a phosphorylcholine-based zwitterionic polymer. However, these surface coatings and surface functionalizations were based on the physical adsorption of proteins and polymers to a PP surface, which might be easily detached by shear stress in the solution.

The use of maleic anhydride-grafted chlorinated polypropylene (MPO or CPO, Fig. 1) is a simple and practical approach for the surface functionalization of PP, which is currently used for painting car bumpers and PP-based commodities [29]. MPO has a polyolefin backbone that is partially maleic anhydride-grafted and chlorinated. The backbone has a high affinity for polyolefin surfaces, and the maleic anhydride-grafted and chlorinated moieties produce hydrogen bonding and dipole–dipole interactions with other substances, making it an adhesion promoter (primer) for enhancing the adhesion of paint and other materials to PP. For instance, Sass and colleagues [30] reported the successful adhesion of MPO to a PP surface, and Treado and colleagues [31] developed a novel fluorescence microscope system to characterize the mechanism of MPO adhesion to PP surfaces. Winnik and colleagues [30, 32] used a laser scanning confocal microscope to study the migration of MPO in the bulk of polyolefins. Although many studies focused on MPO, including patents, have been reported [33–36], there are, to our knowledge, no reports on the surface functionalization of PP using another functional polymer with MPO to introduce antifouling properties or to immobilize a functional molecule on the PP surface.

We previously reported that surface segregation of poly(ethylene glycol) (PEG) chains was achieved when an acrylic substrate was dip-coated with a solution of a methacrylate-based terpolymer containing perfluoroalkyl (R_f)-conjugated monomers and PEGylated monomers [37]. The coated surface simultaneously exhibited significant hydrophobicity, adhesiveness, and low-fouling properties. In this study, we aimed to functionalize a PP surface via dip-coating with a solution of a terpolymer containing R_f groups and PEG chains (PMFP, Fig. 1) in the presence of MPO to produce a low-fouling PP surface that can covalently immobilize a functional molecule. We found that the presence of MPO aided in the adhesion of the terpolymer to the PP surface and that the coated PP surface exhibited low protein-fouling properties. Finally, the dip-coating of a terpolymer containing reactive groups (–COOH) with MPO caused the reactive groups to be presented at an outermost surface, allowing for the

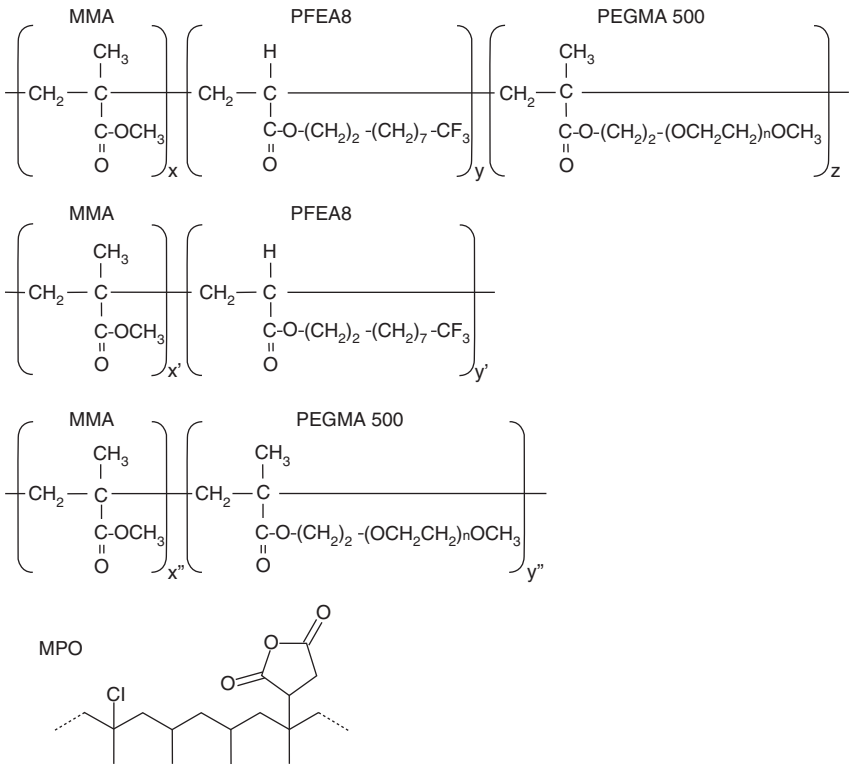

Fig. 1 Chemical structures of a terpolymer containing perfluoroalkyl (R_f)-conjugated monomers and poly(ethylene glycol) monomers (PMFP), poly(MMA-*r*-PFEA8), poly(MMA-*r*-PEGMA500), and modified polyolefin (MPO)

covalent immobilization of a biomolecule on the dip-coated PP surface.

Materials and methods

Materials

Methyl methacrylate (MMA) was purchased from Wako Pure Chemical Industries, Inc. (Osaka, Japan) and was distilled under reduced pressure before use. The fluorine-containing monomer, 2-(perfluorooctyl) ethyl acrylate (PFEA8) was provided by DIC Corp. (Tokyo, Japan) and was used as received. Poly(ethylene glycol) methyl ether methacrylate (PEGMA500) and fluorescein isothiocyanate isomer-I (FITC) were purchased from Sigma-Aldrich (St. Louis, MO). PEGMA500 was used after it was passed through a column packed with activated alumina to remove the stabilizer. Maleic acid-modified chlorinated polyolefin (MPO) (HARDLEN® CY-9124P, $M_n = 3.3 \times 10^4$, $M_w/M_n = 2.0$) was provided by Toyobo Co. Ltd. (Osaka, Japan). Isotactic polypropylene (PP) ($M_n = 640{,}000$, NOBLEN HD 100G2) was provided by Sumitomo Chemical Co. Ltd. (Tokyo, Japan). Amino-dPEG$_8$-*t*-butyl ester was purchased from Quanta BioDesign, Ltd. (Plain City, OH). Cystamine dihydrochloride and tris(2-carboxyethyl) phosphine hydrochloride (TCEP) were purchased from Tokyo Chemical Industry Co. Ltd. (Tokyo, Japan). 1-Ethyl-3-(3-dimethylaminopropyl)carbodiimide, hydrochloride (WSC) was purchased from Dojindo Molecular Technologies Inc. (Kumamoto, Japan). Other chemicals were purchased from Wako Pure Chemical Industries and were used as received.

Preparation of terpolymer containing R_f groups and PEG chains (PMFP)

A terpolymer containing R_f groups and PEG chains [37] (poly(MMA/PFEA8/PEGMA500)) (PMFP) was synthesized by free-radical polymerization in ethyl acetate at 70 °C for 20 h using AIBN as an initiator (0.5% w/w to monomers) under an atmosphere of N_2. The sum of monomer concentrations (MMA, PFEA8, and PEGMA500) was 30% w/w in ethyl acetate. After N_2 bubbling, the polymerization was initiated by the addition of AIBN. After 20 h, the solution was poured into an excess of *n*-hexane at room temperature and was washed twice with an excess of *n*-hexane, followed by drying under a vacuum for 24 h. Synthesized PMFP was obtained as a white precipitate. As controls, the random copolymers poly(MMA/PEGMA500) and poly(MMA/PFEA8) (Fig. 1) were synthesized according to a similar method.

Proton nuclear magnetic resonance (^{1}H-NMR) analysis was performed using an Avance-500 (Bruker BioSpin GmbH, Rheinstetten, Germany) and chloroform-d containing 0.03 wt% tetramethylsilane as a solvent. The chemical shifts of protons assigned to PEG chains and R_f moieties were observed at approximately 3.5 and 4.0 ppm, respectively [38, 39].

PMFP: ^{1}H-NMR (500 MHz, $CDCl_3$): δ (ppm) = 0.80–1.10 (m, 66H), 2.41–2.50 (m, 10H), 4.1 (m, 6H) (Figure S1). The monomer composition ratio (MMA/PFEA8/PEGMA500) was 73:17:10 based on the ^{1}H-NMR results.

Poly(MMA-*r*-PEGMA500): ^{1}H-NMR (500 MHz, $CDCl_3$): δ (ppm) = 3.52 (t, 68H, -CO-CH_2-CH_2-CO-), 1.79–2.10 (m, 20H, -C-CH_2-), and 0.81–1.19 (m, 36H, -C-CH_3) (Figure S2). The monomer composition ratio (MMA/PEGMA500) was 84:16.

Poly(MMA-*r*-PFEA8): ^{1}H-NMR (500 MHz, $CDCl_3$): δ (ppm) = 3.59 (s, 63H, O-CH_3), 2.48–2.52 (m, 10H, -O-CH_2-CH_2-Rf) (Figure S3). The monomer composition (MMA/PFEA8) was 79:21.

The weight-average molecular weight (M_w) and number-average molecular weight (M_n) were measured using a size exclusion chromatograph (SEC) (GPC 8020, Tosoh Corporation, Tokyo, Japan) equipped with a 7.5 × 300 mm SEC column (GF510, Showa Denko K.K., Tokyo, Japan) and a refractive index detector (RI-8031, JASCO, Tokyo, Japan) at 40 °C using tetrahydrofuran as an eluent. Poly(methyl methacrylate) was used for the molecular weight standards. The molecular weight and polydispersity of the synthesized polymer are shown in Table 1.

Dip-coating PP substrates with synthesized polymers

PP substrates (thickness, 0.2 mm) were prepared from PP pellets using a melt-press apparatus (Gonno Koki, Osaka, Japan) and were cut into 1 cm × 1 cm pieces. MPO was used as a matrix resin to immobilize PMFP on the PP surface. First, MPO was dissolved in toluene at 1.0 wt% and was heated (MPO solution). PMFP was then dissolved in an MPO solution at 4.0 wt% (MPO/PMFP solution). A toluene solution containing PMFP 4.0 wt% was also prepared without MPO (PMFP solution). Other polymer solutions were prepared in a similar manner. After stirring the

Table 1 Number-average molecular weights and molecular weight distributions of polymers synthesized in this study

Polymer	M_n	M_w/M_n
PMFP (poly(MMA-*r*-PFEA8-*r*-PEGMA500))	1.0×10^5	1.4
Poly(MMA-*r*-PFEA8)	2.4×10^4	1.6
Poly(MMA-*r*-PEGMA500)	4.8×10^4	1.9

polymer solutions overnight, PP pieces were immersed in the solutions for a few seconds, withdrawn over 2 s (dip-coating), and dried overnight at room temperature under a vacuum.

Stability, wettability, and surface morphology of coated PP surfaces

The stability of the polymer coatings on the PP substrates was investigated by peeling tests using Scotch tape (Nichiban Co. Ltd., Tokyo, Japan, cut into $1 \times 2\ cm^2$). A polymer solution (3 µl) was drop-cast on a PP substrate (coating diameter ~5 mm) and was dried under a vacuum overnight. Scotch tape was applied to a drop-cast surface and then peeled off, and the coated polymer layer was observed with the naked eye.

Contact angle measurements using water and oil droplets (~5 µl) were acquired using a DMs-401 (Kyowa Interface Science Co., Ltd, Niiza, Japan). *n*-Hexadecane was used for the oil droplet contact angle measurements. The measurement was performed for five different substrates, and the reported values are the means of the five measurements. Error bars represent the standard deviations.

The X-ray photoelectron spectroscopy (XPS) measurements were performed with a PHI X-tool X-ray photon spectroscopic instrument (ULVAC, Chigasaki, Japan) using an Al Kα source (15 kV, 4 W). For a wide spectrum, the photoelectron take-off angle was 45°, and spot size was 24 µm × 24 µm. Survey scans were performed with a pass energy of 280 eV and a step size of 0.5 eV. For narrow spectrum using sputtering, the photoelectron take-off angle was 45°, and spot size was 234 µm × 234 µm using an Al Kα source (15 kV, 51 W). Survey scans were performed with a pass energy of 140 and a step size of 0.25 eV. Depth profiling was accomplished using an Ar^+ source at 4.00 keV, and the sputtering was carried in 1 min intervals for a total of 50 min.

Protein adsorption on dip-coated PP surfaces

Bare and dip-coated PP substrates ($1 \times 1\ cm^2$) were immersed in 0.1 M phosphate buffer solution (pH 7.4, 4.0 ml) containing 5.0 mg/ml bovine serum albumin (BSA) for 24 h at 25 °C and were washed with 15 ml of phosphate buffer. The amount of BSA adsorbed on a substrate was measured using a Micro BCA™ Protein Assay Kit (Thermo Fisher Scientific Inc., Waltham, MA).

Introduction of carboxy groups on PP surfaces via dip-coating

The synthesis of a terpolymer containing R_f groups and PEG chains with carboxy ester (*t*-BPEGMA) at their termini (PMFB) is described in the SI (also see Figure S4 and S5). PP surfaces were dip-coated in a similar manner as described above. Briefly, MPO was dissolved in toluene at 1.0 wt % (MPO solution). PMFB was then dissolved in an MPO solution to produce 0.1–4.0 wt% solutions (MPO/PMFB). A PMFB solution was also prepared using toluene without MPO. After stirring the polymer solutions overnight, PP substrates were dip-coated with the solutions and were dried overnight at room temperature under a vacuum.

Quantification of carboxy groups on dip-coated PP surfaces

Carboxy groups protected by *t*-butyl groups on the dip-coated PP surfaces were deprotected with 4 M aqueous HCl (4 mL) at 40 °C overnight to expose the carboxy groups (Figure S6 and S7) [40, 41]. The substrates were then washed three times with Milli-Q water and immersed in a phosphate buffer (0.1 M, pH 8.0, 2 ml) containing 5 vol% dimethyl sulfoxide, 0.6 mM FITC-S-S-NH_2 (see SI), and 5 mM 4-(4,6-dimethoxy-1,3,5-triazin-2-yl)-4-methylmorpholinium chloride (DMT-MM) and were shaken for 2 h at room temperature to conjugate FITC-S-S-NH_2 to the carboxy groups on the dip-coated PP surfaces. The substrates were washed three times with an excess of phosphate buffer and were immersed in an aqueous HCl solution (5 mM, 10 ml) for 1 h at 40 °C with shaking. The HCl solution was replaced with an aqueous NaOH solution (5 mM, 10 ml) and was shaken for 1 h at 40 °C. The NaOH solution was subsequently replaced with an aqueous HCl solution (5 mM, 10 ml) and was shaken for 1 h at 40 °C. Repeated washing with HCl and NaOH solutions was performed to solubilize and remove nonspecifically adsorbed FITC-S-S-NH_2. Finally, the substrates were rinsed with phosphate buffer and were immersed in a phosphate buffer (0.1 M, pH 8.0, 2 ml) containing 2 mM TCEP for 1 h with shaking at 40 °C, which facilitated the release of the fluorophore into the solution phase. The fluorescence intensity of the phosphate buffer was measured using a fluorescence spectrophotometer (FP-8200, JASCO, Tokyo, Japan). The measurements were repeated three times, and averaged data are presented with error bars (standard deviations). A standard curve for the liberated fluorophore is shown in Figure S8.

Results and discussion

Drop-casting synthesized polymer solutions on PP substrates

PP has a remarkably low surface energy, which makes it difficult to immobilize another polymer on its surface.

One of the rational and simple approaches to immobilizing another polymer on PP is to use MPO. MPO can be used in two ways: precoating MPO on a PP surface or coating with a mixture of MPO and another polymer. In the present study, we adopted the latter approach because it can minimize and simplify the process of PP surface functionalization. To test the adhesion of the coated polymer layer to the PP surface, we cast a droplet of a polymer solution on a PP surface (drop-casting). Figure 2 shows photos of drop-cast PP substrates before and after a peeling test. Drop-cast PMFP and MPO/PMFP were visible to the naked eye after drying (Fig. 2a–c). In the case of only using PMFP (Fig. 2b), the casted PMFP layer was removed readily by the peeling test. In the case of a mixture of MPO/PMFP (Fig. 2c), the MPO/PMFP on the PP substrate remained after the peeling test, indicating that a mixture of MPO and PMFP was stably immobilized on the PP surface.

XPS analysis of dip-coated PP surfaces

The surfaces of the dip-coated PP substrates were evaluated using XPS measurements. Figure 3 shows XPS spectra of the surfaces of bare and dip-coated PP substrates. While the

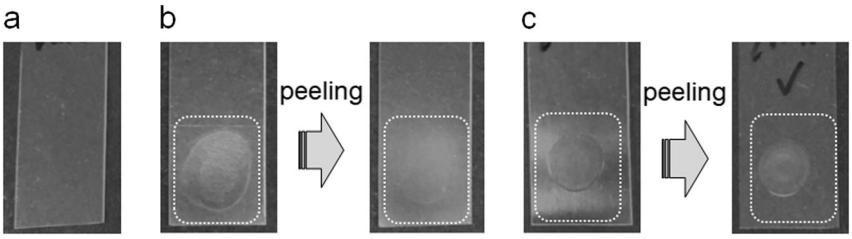

Fig. 2 Optical images of Scotch tape-peeling tests for PP substrates. **a** Bare PP, **b** PP drop-cast with a PMFP solution, and **c** PP drop-cast with a MPO/PMFP solution. Polymer solution (3 µl) was drop-cast on the PP substrate (coating diameter was approximately 5 mm) and was dried under a vacuum overnight

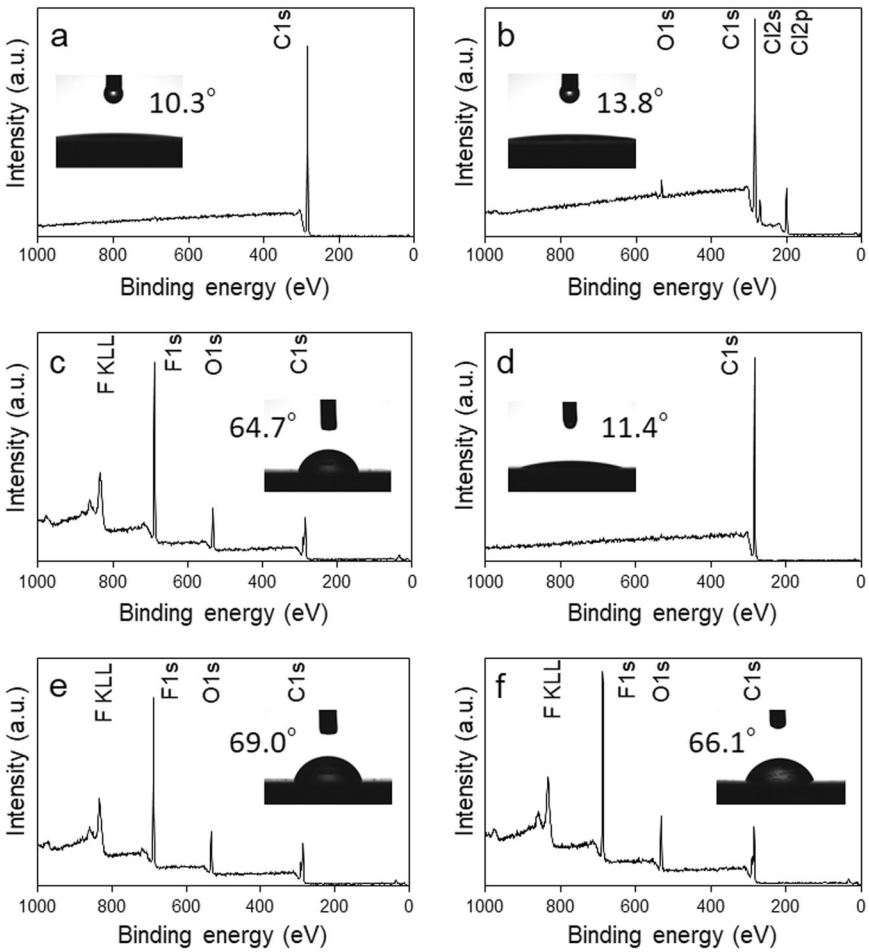

Fig. 3 XPS spectra of bare and dip-coated PP surfaces. Insets are optical images of oil contact angle measurements. **a** Bare PP, **b** PP dip-coated with MPO after the peeling test, **c** PP dip-coated with PMFP before the peeling test, **d** PP dip-coated with PMFP after the peeling test, **e** PP dip-coated with MPO/PMFP before the peeling test, and **f** PP dip-coated with MPO/PMFP after the peeling test

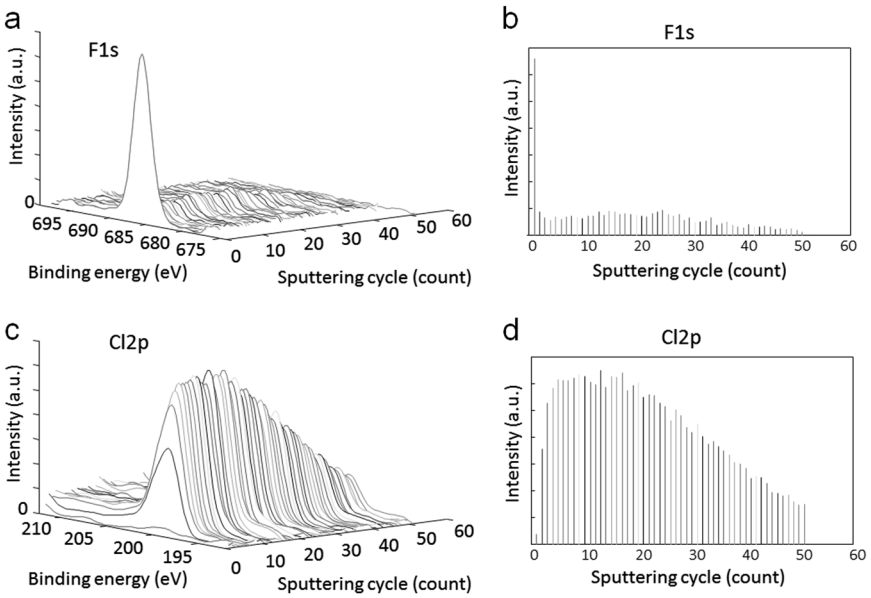

Fig. 4 XPS depth profiles of a PP surface dip-coated with MPO/PMFP. **a**, **b** F_{1s} and **c**, **d** Cl_{2p}. Atomic intensities are shown as a function of sputtering cycle

surface of a bare PP substrate exhibited only a C_{1s} peak, the spectrum of PP dip-coated with MPO shows O_{1s}, Cl_{2s}, and Cl_{2p} peaks (Fig. 3b), suggesting that MPO remained on the PP surface after the peeling test. Although Fig. 3c shows F_{kll}, F_{1s}, and O_{1s} peaks that were derived from PMFP, for the PP substrate dip-coated with PMFP before the peeling test, Fig. 3d shows no fluorine or oxygen-derived peaks (after the peeling test), demonstrating that PMFP did not adhere to the PP surface in the absence of MPO and was easily removed by the peeling test. Oil contact angle measurements (insets of Fig. 3) showed that the PMFP dip-coating made the PP surface oleophobic and that the peeling test caused it to revert back to being oleophilic, which also suggests the removal of PMFP from the surface. Dip-coating with an MPO/PMFP solution produced F_{kll}, F_{1s}, and O_{1s} peaks in the XPS spectra before and after the peeling test (Fig. 3e, f). It should be noted that the Cl_{2p} peak was not observed. Since MPO contained Cl atoms, the disappearance of Cl in the XPS spectrum indicates the absence of MPO on the outermost surface, suggesting the segregation of PMFP on the outermost surface. The oil contact angle measurements also showed the oil repellency of the surface that was dip-coated with the MPO/PMFP solution before and after the peeling test. These results indicate that PMFP was stably immobilized on the PP surface in the presence of MPO and that PMFP was predominantly segregated on the surface of the dip-coated polymer layer. The surface segregation of PMFP is expected to be induced by the R_f groups in PMFP [37].

The surface was sputtered using an Ar-ion laser to obtain depth profiles of the dip-coated polymer layer (Fig. 4). Sputtering was repeated in 1 min intervals, and the sputtering cycles were supposed to be proportional to the depth from the outermost surface. Although the F_{1s} peak had a high intensity at the outermost surface, the F_{1s} peak decreased drastically after the single sputtering (Fig. 4a, b). Until 25 cycles of sputtering were performed, the F_{1s} peak intensity was low but obviously detected. After 25 cycles of sputtering, the F_{1s} peak decreased with the sputtering cycle. Figure 4c, d shows the depth profile of Cl element. While the Cl_{2p} peak, which was derived from MPO, was almost negligible at the outermost surface, the Cl_{2p} peak intensity increased with the sputtering cycle up to approximately 15 cycles and then gradually decreased. The depth profiles of F_{1s} and Cl_{2p} clearly demonstrate the surface segregation of PMFP.

Since approximately 40 cycles of sputtering would reach the original PP surface according to the thickness of the coated polymer layer (~0.4 μm, discussed later) and the sputtering speed, these results indicate that the MPO was penetrated to an original PP substrate to blur the boundary between the original PP surface and the coated polymer layer. This is one of the mechanisms for adhesion of the coated polymer to a PP surface. The methacrylate-based copolymers (PMFP and others) appeared to be macroscopically miscible with MPO, and the XPS depth profile also indicates a relatively homogeneous distribution of MPO in the coated polymer layer (except for the outermost layer), although it was possible that microphase separation occurred in the coated polymer layer. The methacrylate-based polymer backbone might have contributed to the compatibility with MPO. Indeed, the following section

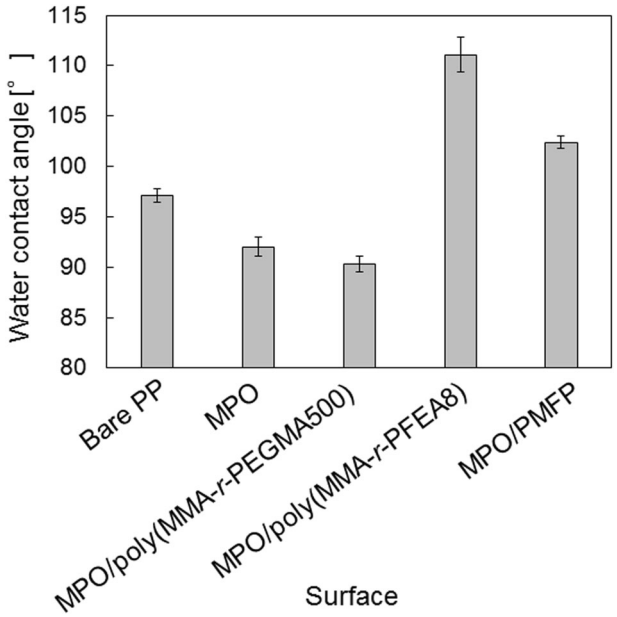

Fig. 5 Water contact angle measurements for bare and dip-coated PP surfaces

reveals the successful coating of poly(MMA-*r*-PEGMA500) and poly(MMA-*r*-PFEA8) on PP surfaces in the presence of MPO.

Wettability of dip-coated PP surfaces

Wettability is an important surface property. Figure 5 shows the static water contact angles of the PP surfaces. Dip-coating with an MPO solution and a mixture of MPO/poly (MMA-*r*-PEGMA500) produced water contact angles that were slightly lower than those of the bare PP substrate, which could be due to the polar moieties in MPO and poly (MMA-*r*-PEGMA500). Dip-coating with a poly(MMA-*r*-PFEA8) solution resulted in a water contact angle of 111°, which was likely to be caused by surface segregation of the R_f groups in the dip-coated layer. Dip-coating with a mixture of MPO/PMFP also showed a high water contact angle, which was slightly lower than that of poly(MMA-*r*-PFEA8). The relatively high water contact angle for the surface that was dip-coated with MPO/PMFP indicated the presence of R_f groups and PEG moieties on the outermost surface. We previously demonstrated the surface segregation of R_f groups accompanied with PEG moieties [42] and showed that the R_f group content affected surface segregation [41]. The content of R_f -conjugated monomers in poly (MMA-*r*-PFEA8) and PMFP was 21 and 17%, respectively. The slightly low composition of R_f groups in PMFP could result in reduced surface segregation of R_f groups, and the presence of PEG chains would affect surface hydrophobicity.

Table 2 Root mean square (RMS) roughness of dip-coated PP surfaces

Surface	RMS roughness (nm)
Bare PP surface	8.0
MPO-coated surface	1.2
MPO/poly(MMA-*r*-PEGMA)-coated surface	5.4
MPO/poly(MMA-*r*-PFEA8)-coated surface	0.9
MPO/PMFP-coated surface	2.7

AFM imaging of dip-coated PP surfaces

The thickness was determined from the average weight change of the substrates (more than 20 pieces), assuming that the PMFP density was similar to that of PMMA (1.18 g/cm^3) and the MPO density was 1.05 g/cm^3 (manufacturer information). The thickness of the dip-coated MPO/PMFP layer was typically found to be 0.4 μm, which was prepared with a toluene solution containing 1.0 wt% MPO and 1.0 wt% PMFP. The surface morphologies of the bare and dip-coated PP substrates were investigated using atomic force microscopy (AFM) (Figure S9). The bare PP surface had stripe-like morphology, which resulted from the surface of the melt press. Dip-coating with MPO resulted in a surface characterized by small nodules, and dip-coating with MPO/poly(MMA-*r*-PEGMA) resulted in a surface characterized by relatively large nodules. Dip-coating with MPO/poly(MMA-*r*-PFEA8) created a remarkably flat surface, whereas dip-coating with MPO/PMFP resulted in an undulating surface. Based on the AFM images, root mean square (RMS) roughness values of the surfaces were calculated and are summarized in Table 2. While a bare PP surface had a roughness of 8 nm, dip-coating with polymers reduced this roughness. Because all of the roughness values were less than 10 nm, we concluded that these surfaces were sufficiently flat to be compared to one another. The low roughness of these dip-coated surfaces agreed with the transparency of the dip-coated substrates.

Fouling properties of dip-coated PP substrates

We previously reported that a PMFP-derivative dip-coating on an acrylic substrate induced surface segregation of the R_f groups and PEG chains in the polymer, in which PMFP was stably immobilized on an acrylic substrate in the absence of MPO [37]. The surface segregation produced a surface with low nonspecific protein adsorption. Here, we also investigated the fouling properties of dip-coated PP surfaces. Fouling properties were evaluated from the amount of BSA adsorbed on dip-coated PP surfaces. Figure 6 shows the amount of BSA adsorption on bare and dip-coated PP surfaces. While a bare PP surface adsorbed approximately 0.9 μg/cm^2 of BSA, dip-coating with MPO and MPO/poly

(MMA-*r*-PEGMA500) solutions increased the BSA adsorption to approximately 1.2 μg/cm^2. These results indicate that MPO and MPO/poly(MMA-*r*-PEGMA500) surfaces are more likely to adsorb BSA compared to a bare PP surface. In the case of the MPO/poly(MMA-*r*-PEGMA500) dip-coating, it is possible that the PEG chains were buried in the bulk of the dip-coated polymer layer due to the surface segregation of hydrophobic moieties in MPO and poly(MMA-*r*-PEGMA500). Dip-coating with MPO/poly(MMA-*r*-PFEA8) reduced the BSA adsorption to approximately 0.5 μg/cm^2, which could be due to the R_f groups that were present on the surface. Dip-coating with a mixture of MPO/PMFP further reduced the BSA adsorption, which was one-third of the adsorption of bare PP. This low-fouling property indicates surface segregation of not only the R_f groups but also the PEG chains in PMFP, which is consistent with our previous report [37]. These results suggest that MPO/PMFP dip-coating is effective for reducing the nonspecific protein adsorption to PP surfaces.

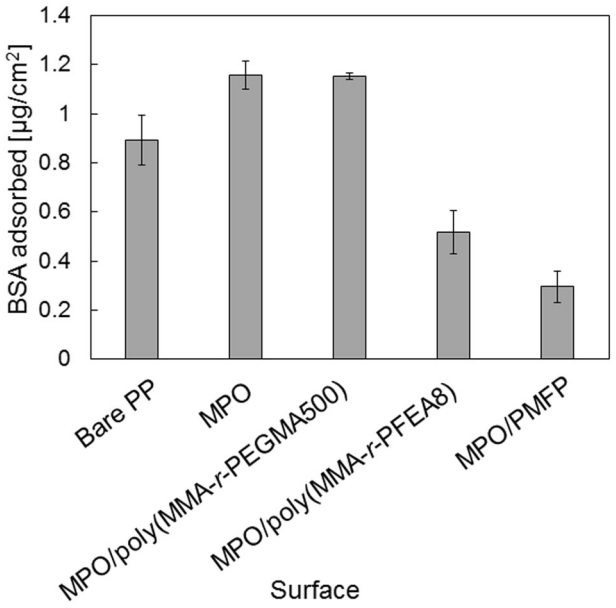

Fig. 6 Amount of BSA adsorbed on bare and dip-coated PP surfaces

Introduction of carboxy groups on PP surfaces by dip-coating with PMFB

The above investigations demonstrated that dip-coating with a mixture of MPO and a methacrylate-based terpolymer immobilized the terpolymer on a PP surface. We then tried to introduce carboxy groups onto a dip-coated PP surface, which could subsequently be used to immobilize functional molecules onto the surface via covalent bonds. To this end, we synthesized another terpolymer (PMFB, Fig. 7a) composed of MMA, PFEA8, and *t*-BPEGMA monomers. The M_w of PMFB was 2.1×10^4, and the M_w/M_n was 1.8. Elemental analysis revealed that the monomer composition ratio (MMA/PFEA8/*t*-BPEGMA) was 72:15:13.

After dip-coating a PP substrate with a mixture of MPO/PMFB, carboxy groups on the PP surface were exposed by deprotection of the *tert*-butyl esters using 4 M HCl_{aq} at 40 °C. A cleavable fluorescent compound (FITC-S-S-NH_2) was used to quantify the surface density of carboxy groups on the dip-coated PP surfaces (Scheme S1) [41]. FITC-S-S-NH_2 has a reactive amine group and a cleavable disulfide bond. FITC-S-S-NH_2 was conjugated to the carboxy groups

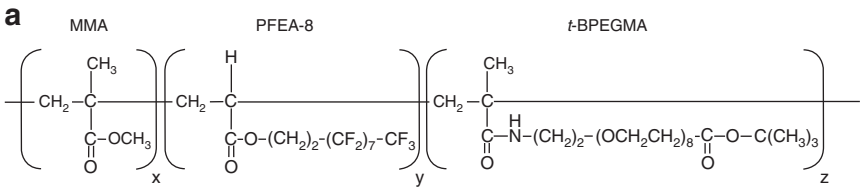

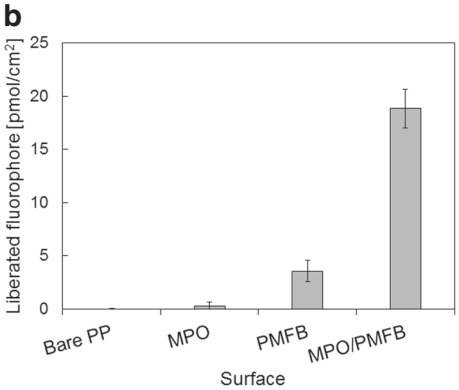

Fig. 7 **a** Chemical structure of poly(MMA-*r*-PFEA8-*r*-*t*-BPEGMA) (PMFB). **b** Surface density of carboxy groups on PP dip-coated with various polymers. Each polymer was used at 1.0 wt% in toluene

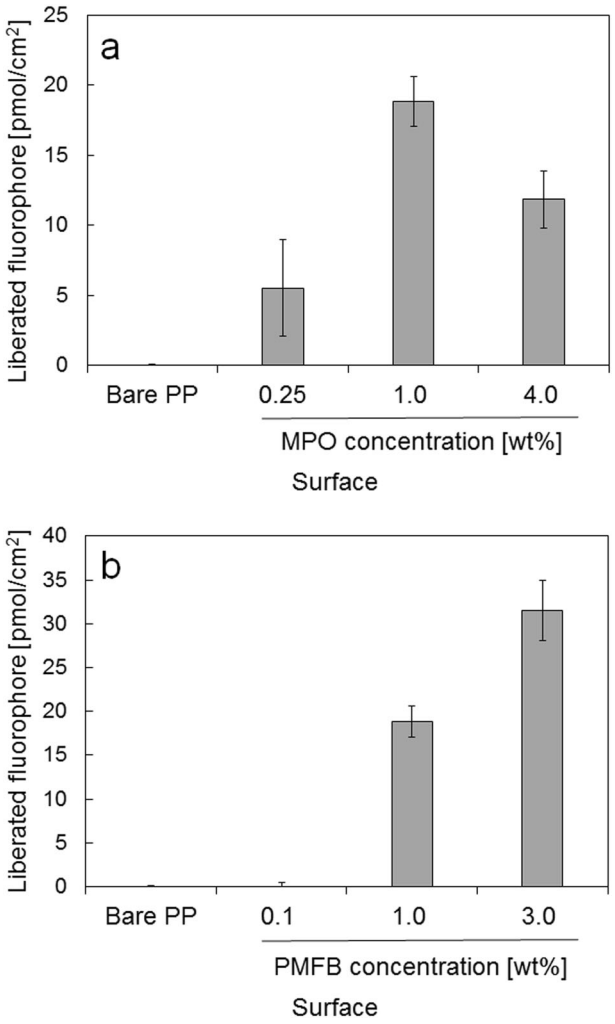

Fig. 8 Surface density of carboxy groups on PP surfaces dip-coated with a mixture solution of MPO/PMFB. **a** Effect of MPO concentration (PMFB concentration was 1.0 wt%). **b** Effect of PMFB concentration (MPO concentration was 1.0 wt%)

on the surface in the presence of a condensation agent. The fluorophore was liberated to solution upon the reduction of the disulfide bond. Thus, the amount of immobilized fluorescent compound could be quantified using a conventional fluorescence spectrophotometer [43, 44]. Figure 7b shows that bare and MPO-coated PP surfaces did not have carboxy groups for conjugation. The PMFB-coated PP surface had only a small amount of carboxy groups, probably because the dip-coating with PMFB failed to form a stable PMFB layer on the PP surface. The surface dip-coated with a mixture of MPO/PMFB had carboxy groups with a density of approximately 19 pmol/cm^2, which is comparable to our previous report [41]. It should be noted that the layer of coated MPO/PMFB was not detached from the PP surface during the quantification process, which involved numerous washing steps. These results demonstrate that dip-coating with MPO/PMFB resulted in the

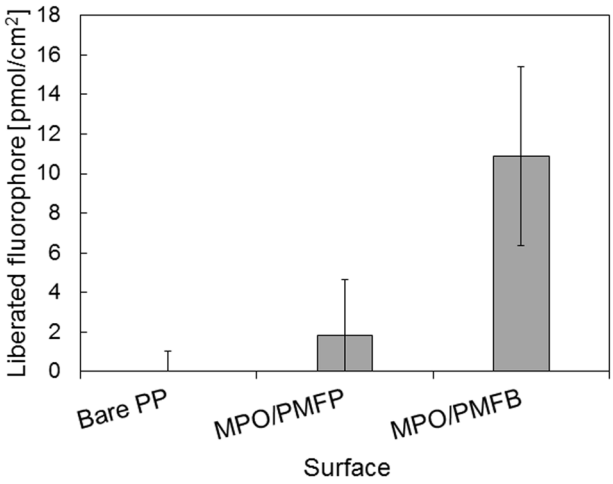

Fig. 9 Amount of HRP immobilized on PP dip-coated with polymers

successful presentation of carboxy groups on the dip-coated surface and that the carboxy groups were accessible for solutes in an aqueous solution.

The effects of the MPO and PMFB concentrations on the surface density of carboxy groups were investigated (Fig. 8). The dip-coating with a mixture of 1.0 wt% MPO and 1.0 wt% PMFB had the highest surface density, and the coating that had a high MPO concentration (4.0 wt%) had a low density (Fig. 8a), which may be due to the decrease in the PMFB composition of the polymer mixture. As the PMFB concentration increased, the surface density of carboxy groups increased (Fig. 8b).

Immobilization of biomolecules on dip-coated PP surfaces

The covalent immobilization of functional biomolecules and ligands on a low-fouling surface is of great importance for biosensors and medical devices because it can improve signal-to-noise ratios in detection [45–48]. We attempted to immobilize an enzyme on a PP surface that was dip-coated with PMFB using carboxy groups as reactive sites. PP substrates that were dip-coated with an MPO/PMFB mixture (1.0 wt%/1.0 wt% in toluene) were used for horseradish peroxidase (HRP) immobilization. HRP is one of the major enzymes that is used for various biosensors, and it has two amino groups on its surface. Carboxy groups displayed on the dip-coated surface were reacted with *N*-hydroxysuccinimide in the presence of a condensation agent, and then HRP was conjugated to the surface. Figure 9 shows that HRP (~11 pmol/cm^2) was successfully immobilized on the MPO/PMFB-coated PP surface, whereas negligible amounts of HRP were immobilized on bare or PMFP-coated PP surfaces. It should be noted that in the absence of a condensation agent, HRP was not immobilized on the MPO/PMFB-coated PP surface.

We examined the HRP activity immobilized on surfaces. 2,2'-Azino-bis(3-ethylbenzothiazoline-6-sulfonic acid) (ABTS) was used as an enzyme substrate in the presence of hydrogen peroxide. Figure S10 shows the time courses of the oxidation of ABTS catalyzed by HRP immobilized on surfaces. A bare PP surface treated with HRP catalyzed the reaction to some extent, probably due to the nonspecific adsorption of HRP on a bare PP surface. The PMFP-coated surface treated with HRP and the PFMB-coated surface (without HRP) did not catalyze the reaction, indicating the absence of HRP on their surfaces. The PMFB-coated surface treated with HRP catalyzed the reaction, indicating that immobilized HRP was active on the surface. These results demonstrate the covalent immobilization of HRP on the MPO/PMFB-coated PP surface and its resulting low-fouling properties, which supports the results that are shown in Fig. 6.

Conclusion

In general, the surface functionalization of PP is still challenging. The remarkably low surface energy of PP prevents the adhesion of other polymers on a PP surface. In the present study, we used an MPO/methacrylate-based terpolymer mixture to functionalize a PP surface via dip-coating. MPO was used to successfully immobilize a methacrylate-based terpolymer (PMFP) on a PP surface. XPS, contact angle, and protein adsorption measurements revealed that the R_f groups and PEG chains in PMFP were segregated to the outermost surface of the dip-coated layer. The surface segregation of these moieties produced a low-fouling surface on the PP substrate. PMFB, which is a terpolymer that contains R_f groups and PEG chains with carboxy groups at their termini, was also dip-coated on a PP substrate. The surface segregation induced the presentation of carboxy groups on the outermost surface, and their density was quantified to be approximately 20 pmol/cm^2. Finally, the carboxy groups were successfully used as reactive sites for immobilizing a protein, facilitating protein immobilization on a low-fouling surface. The present study demonstrates that a functional methacrylate-based polymer was readily and stably coated on a PP surface with the aid of MPO and that the control of the surface segregation of side chains in the polymer created a functionalized outermost surface on the PP substrate, which could lead to PP-based biosensors and biocompatible medical devices. As polyolefins are widely used in industry and daily life, the strategy presented herein will extend the potential of polyolefin surfaces and will provide polyolefin surfaces functionalized with other polymers, ligands, and biomolecules.

Acknowledgements The authors thank Professor A Mori, Professor H Minami, and Professor A Kondo (Kobe Univ.) for technical assistance. This study was financially supported by the Special Coordination Funds for Promoting Science and Technology, Creation of Innovation Centers for Advanced Interdisciplinary Research Areas (Innovative Bioproduction Kobe), MEXT, Japan, by JSPS KAKENHI Grant Numbers 16H04577, 18K18976, and 18H04566.

Compliance with ethical standards

Conflict of interest The authors declare that they have no conflict of interest.

Publisher's note: Springer Nature remains neutral with regard to jurisdictional claims in published maps and institutional affiliations.

References

1. Brockman JM, Frutos AG, Corn RM. A multistep chemical modification procedure to create DNA arrays on gold surfaces for the study of protein-DNA interactions with surface plasmon resonance imaging. J Am Chem Soc. 1999;121:8044–51.
2. Hergenrother PJ, Depew KM, Schreiber SL. Small-molecule microarrays: covalent attachment and screening of alcohol-containing small molecules on glass slides. J Am Chem Soc. 2000;122:7849–50.
3. Korbel GA, Lalic G, Shair MD. Reaction microarrays: a method for rapidly determining the enantiomeric excess of thousands of samples. J Am Chem Soc. 2001;123:361–2.
4. Reyes DR, Iossifidis D, Auroux PA, Manz A. Micro total analysis systems. 1. Introduction, theory, and technology. Anal Chem. 2002;74:2623–36.
5. Pellois JP, Zhou X, Srivannavit O, Zhou T, Gulari E, Gao X. Individually addressable parallel peptide synthesis on microchips. Nat Biotechnol. 2002;20:922–6.
6. Jonkheijm P, Weinrich D, Schroder H, Niemeyer CM, Waldmann H. Chemical strategies for generating protein biochips. Angew Chem Int Ed. 2008;47:9618–47.
7. Hu LZ, Xu GB. Applications and trends in electrochemiluminescence. Chem Soc Rev. 2010;39:3275–304.
8. Scarano S, Mascini M, Turner APF, Minunni M. Surface plasmon resonance imaging for affinity-based biosensors. Biosens Bioelectron. 2010;25:957–66.
9. Aizenshtein EM. Global output of chemical fibres in 2014. Fibre Chem. 2016;48:90–3.
10. Genis AV. Analysis of the global and russian markets of polypropylene and of its main consumption areas. Russ J Gen Chem. 2017;87:2137–50.
11. Hata T, Kitazaki Y, Saito T. Estimation of the surface-energy of polymer solids. J Adhes. 1987;21:177–94.
12. Schadock-Hewitt AJ, Bruce TF, Marcus RK. Evidence for the intercalation of lipid acyl chains into polypropylene fiber matrices. Langmuir. 2015;31:10418–25.
13. Cui NY, Brown NMD. Modification of the surface properties of a polypropylene (pp) film using an air dielectric barrier discharge plasma. Appl Surf Sci. 2002;189:31–8.
14. Schroeder M, Fatarella E, Kovac J, Guebitz GM, Kokol V. Laccase-induced grafting on plasma-pretreated polypropylene. Biomacromolecules. 2008;9:2735–41.
15. Farris S, Pozzoli S, Biagioni P, Duo L, Mancinelli S, Piergiovanni L. The fundamentals of flame treatment for the surface activation of polyolefin polymers - a review. Polym (Guildf). 2010;51:3591–605.
16. Tao GL, Gong AJ, Lu JJ, Sue HJ, Bergbreiter DE. Surface functionalized polypropylene: synthesis, characterization, and adhesion properties. Macromolecules. 2001;34:7672–9.

17. Thompson DB, Trebicky T, Crewdson P, McEachran MJ, Stojcevic G, Arsenault G et al. Functional polymer laminates from hyperthermal hydrogen induced cross-linking. Langmuir. 2011;27:14820–7.
18. Zhao J, Song LJ, Shi Q, Luan SF, Yin JH. Antibacterial and hemocompatibility switchable polypropylene nonwoven fabric membrane surface. ACS Appl Mater Interf. 2013;5:5260–8.
19. Wang H, Wu JJ, Cai C, Guo J, Fan HS, Zhu CZ et al. Mussel inspired modification of polypropylene separators by catechol/polyamine for li-ion batteries. ACS Appl Mater Interf. 2014;6:5602–8.
20. Thakur VK, Vennerberg D, Kessler MR. Green aqueous surface modification of polypropylene for novel polymer nanocomposites. ACS Appl Mater Interf. 2014;6:9349–56.
21. Ozcam AE, Efimenko K, Spontak RJ, Fischer DA, Genzer J. Multipurpose polymeric coating for functionalizing inert polymer surfaces. ACS Appl Mater Interf. 2016;8:5694–705.
22. Kou RQ, Xu ZK, Deng HT, Liu ZM, Seta P, Xu YY. Surface modification of microporous polypropylene membranes by plasma-induced graft polymerization of alpha-allyl glucoside. Langmuir. 2003;19:6869–75.
23. Yang Q, Xu ZK, Dai ZW, Wang JL, Ulbricht M. Surface modification of polypropylene microporous membranes with a novel glycopolymer. Chem Mater. 2005;17:3050–8.
24. Yan MG, Liu LQ, Tang ZQ, Huang L, Li W, Zhou J et al. Plasma surface modification of polypropylene microfiltration membranes and fouling by BSA dispersion. Chem Eng J. 2008;145:218–24.
25. Yang YF, Li Y, Li QL, Wan LS, Xu ZK. Surface hydrophilization of microporous polypropylene membrane by grafting zwitterionic polymer for anti-biofouling. J Membr Sci. 2010;362:255–64.
26. Xin ZR, Yan SJ, Ding JT, Yang ZF, Du BB, Du SS. Surface modification of polypropylene nonwoven fabrics via covalent immobilization of nonionic sugar-based surfactants. Appl Surf Sci. 2014;300:8–15.
27. Salas C, Genzer J, Lucia LA, Hubbe MA, Rojas OJ. Water-wettable polypropylene fibers by facile surface treatment based on soy proteins. ACS Appl Mater Interf. 2013;5:6541–8.
28. Chen SH, Chang Y, Ishihara K. Reduced blood cell adhesion on polypropylene substrates through a simple surface zwitterionization. Langmuir. 2017;33:611–21.
29. Boaen NK, Hillmyer MA. Post-polymerization functionalization of polyolefins. Chem Soc Rev. 2005;34:267–75.
30. Clemens RJ, Batts GN, Lawniczak JE, Middleton KP, Sass C. How do chlorinated poly(olefins) promote adhesion of coatings to poly(propylene). Prog Org Coat. 1994;24:43–54.
31. Morris HR, Munroe B, Ryntz RA, Treado PJ. Fluorescence and Raman chemical imaging of thermoplastic olefin (TPO) adhesion promotion. Langmuir. 1998;14:2426–34.
32. Ma YC, Winnik MA, Yaneff PV, Ryntz RA. Surface and interface characterization of chlorinated polyolefin coated thermoplastic polyolefin. Jct Res. 2005;2:407–16.
33. Yamamoto N, Yoda M, Wada S. Process for the production of modified polyolefin. US Patent 1979:4146529.
34. Yang JY, Garton A. Primers for adhesive bonding to polyolefins. J Appl Polym Sci. 1993;48:359–70.
35. Singh SK, Tambe SP, Samui AB, Raja VS, Kumar D. Maleic acid grafted low density polyethylene for thermally sprayable anticorrosive coatings. Prog Org Coat. 2006;55:20–6.
36. Kato M, Usuki A, Hasegawa N, Okamoto H, Kawasumi M. Development and applications of polyolefin- and rubber-clay nanocomposites. Polym J. 2011;43:583–93.
37. Tokuda K, Noda M, Maruyama T, Kotera M, Nishino T. A low-fouling polymer surface prepared by controlled segregation of poly(ethylene oxide) and its functionalization with biomolecules. Polym J. 2015;47:328–33.
38. Koda Y, Terashima T, Sawamoto M. LCST-type phase separation of poly[poly(ethylene glycol) methyl ether methacrylate]s in hydrofluorocarbon. ACS Macro Lett. 2015;4:1366–9.
39. Koda Y, Terashima T, Sawamoto M. Multimode self-folding polymers via reversible and thermoresponsive self-assembly of amphiphilic/fluorous random copolymers. Macromolecules. 2016;49:4534–43.
40. Yamamoto S, Kitahata S, Shimomura A, Tokuda K, Nishino T, Maruyama T. Surfactant-induced polymer segregation to produce antifouling aurfaces via dip-coating with an amphiphilic polymer. Langmuir. 2015;31:125–31.
41. Nishimori K, Kitahata S, Nishino T, Maruyama T. Controlling surface-segregation of a polymer to display carboxy groups on an outermost surface using perfluoroacyl group. Langmuir. 2018;34:6396–404.
42. Tokuda K, Kawasaki M, Kotera M, Nishino T. Highly water repellent but highly adhesive surface with segregation of poly (ethylene oxide) side chains. Langmuir. 2015;31:209–14.
43. Shimomura A, Nishino T, Maruyama T. Display of amino groups on substrate surfaces by simple dip-coating of methacrylate-based polymers and its application to DNA immobilization. Langmuir. 2013;29:932–8.
44. Shiota S, Yamamoto S, Shimomura A, Ojida A, Nishino T, Maruyama T. Quantification of amino groups on solid surfaces using cleavable fluorescent compounds. Langmuir. 2015;31:8824–9.
45. Patel N, Davies MC, Hartshorne M, Heaton RJ, Roberts CJ, Tendler SJB et al. Immobilization of protein molecules onto homogeneous and mixed carboxylate-terminated self-assembled monolayers. Langmuir. 1997;13:6485–90.
46. Lahiri J, Isaacs L, Tien J, Whitesides GM. A strategy for the generation of surfaces presenting ligands for studies of binding based on an active ester as a common reactive intermediate: a surface plasmon resonance study. Anal Chem. 1999;71:777–90.
47. Jiang SY, Cao ZQ. Ultralow-fouling, functionalizable, and hydrolyzable zwitterionic materials and their derivatives for biological applications. Adv Mater. 2010;22:920–32.
48. Sung D, Park S, Jon S. Facile immobilization of biomolecules onto various surfaces using epoxide-containing antibiofouling polymers. Langmuir. 2012;28:4507–14.